Cell. Mol. Biol. (ISSN: 1165-158X)

Journal Homepage: www.cellmolbiol.org

Cellular and Molecular Biology

Original Article

Homocysteine modulates CXCL10/CXCR3 axis activity to induce endothelial dysfunction

Yanjie Xu[1], Yingying Xu[1], Zuozong Yu[1], Dingwen He[2*]

[1] *Department of Cardiovascular Medicine, The Second Affiliated Hospital of Nanchang University, Nanchang, Jiangxi 330006, China*

[2] *Department of Orthopaedics, The Second Affiliated Hospital of Nanchang University, Nanchang, Jiangxi 330006, China*

Article Info

Article history:

Received: September 11, 2023
Accepted: December 19, 2023
Published: February 29, 2024

Use your device to scan and read the article online

Abstract

Elevated homocysteine (Hcy) levels have been linked to the development of cardiovascular diseases, notably endothelial dysfunction, a critical precursor to atherosclerosis. In this extensive investigation, we explore the intricate pathways through which Hcy influences endothelial dysfunction, with particular attention to the CXCL10/CXCR3 axis. Employing a dual approach encompassing both in vitro and in vivo models, we scrutinize the repercussions of Hcy exposure on endothelial functionality. Our results reveal that Hcy significantly impairs crucial endothelial processes, including cell migration, proliferation, and tube formation. Concomitantly, Hcy upregulates the expression of adhesion molecules, exacerbating endothelial dysfunction. In a murine hyperhomocysteinemia (HHcy) model, we observed a parallel increase in plasma Hcy levels and adverse vascular effects. Moreover, our study unraveled a pivotal role of the CXCL10/CXCR3 axis in Hcy-induced endothelial dysfunction. Hcy exposure led to the upregulation of CXCL10 and CXCR3, both in vitro and in HHcy mice. Importantly, the blockade of this axis, achieved through specific antibodies or NBI-74330, mitigated the detrimental effects of Hcy on endothelial function. In conclusion, our findings illuminated the central role of the CXCL10/CXCR3 axis in mediating Hcy-induced endothelial dysfunction, providing valuable insights for potential therapeutic strategies in managing HHcy-related cardiovascular diseases.

Keywords: CXCL10, CXCR3, Endothelial dysfunction, Hyperhomocysteinemia

1. Introduction

Endothelial dysfunction serves as a pivotal early event in the initiation of atherosclerosis and other vascular maladies. Its hallmark features include a shift in endothelial behavior, marked by diminished vasodilation, heightened proinflammatory tendencies, and an inclination towards proliferation and prothrombotic properties [1]. Among the factors implicated in driving endothelial dysfunction, Homocysteine (Hcy), a sulfur-containing amino acid stemming from methionine metabolism, stands prominent [2]. Elevated Hcy levels, a condition termed hyperhomocysteinemia (HHcy), have consistently surfaced in association with an augmented susceptibility to cardiovascular disorders [3]. Due to the genetic background and dietary habits of the population, the incidence of elevated blood Hcy levels in China is much higher than that in Western populations [4], greatly increasing the risk of coronary heart disease.

The chemokine CXCL10 and its receptor CXCR3 have been identified as key players in various inflammatory diseases and are involved in the recruitment and activation of leukocytes, contributing to the inflammatory response [5]. Recent studies have suggested that this axis may also play a role in endothelial dysfunction [6], although the exact mechanisms remain unclear. CXCL10, also known as Interferon Gamma-Induced Protein 10 (IP-10), is a small protein that belongs to the 'inflammatory' chemokine family [7]. It binds to its receptor CXCR3, triggering a cascade of reactions that lead to the activation and recruitment of leukocytes such as T cells, eosinophils, monocytes, and natural killer (NK) cells [8]. On the other hand, CXC chemokine receptor 3 (CXCR3) represents a transmembrane receptor belonging to the G protein-coupled receptor family, with its unique ability to selectively engage with CXCL9, CXCL10, and CXCL11 [9]. This receptor finds its primary residence on immune cells, notably activated T lymphocytes and natural killer cells, where it assumes a pivotal role in orchestrating critical immunological functions such as facilitating the homing of effector cells to infection sites for effective pathogen clearance [10].

Hcy is a sulfur-containing amino acid that is produced in the body during the metabolism of methionine, an essential amino acid taken in through the diet [11]. It is normally present in the blood in small amounts [12]. Nonetheless, heightened concentrations of Hcy, manifesting as HHcy,

* Corresponding author.
E-mail address: hedingwen@126.com (D. He).
Doi: http://dx.doi.org/10.14715/cmb/2024.70.2.28

have been linked to arterial damage and an escalated susceptibility to blood clot formation [13]. This is because high levels of Hcy can cause inflammation in the blood vessels, leading to atherosclerosis, which is a hardening and narrowing of the arteries [14]. Therefore, maintaining healthy Hcy levels is important for cardiovascular health.

In this investigation, our primary objective is to delve into the complex interplay between Hcy and the CXCL10/CXCR3 axis. We hypothesize that Hcy can modulate the expression of CXCL10 and CXCR3, thereby contributing to endothelial dysfunction. This study will offer novel perspectives on the function of Hcy and the CXCL10/CXCR3 axis in endothelial dysfunction and highlight potential therapeutic strategies for managing conditions associated with elevated Hcy levels.

2. Materials and methods

2.1. Patient sample

Patient samples were collected in strict adherence to ethical protocols, and comprehensive written informed consent was diligently obtained from all participating individuals. The patient sample cohort was meticulously selected, adhering to ethical guidelines, and obtaining informed consent. Blood samples were collected aseptically from patients and healthy controls, processed promptly, and plasma stored at ultra-low temperatures. Patients were chosen based on documented elevated Hcy levels (≥15 μmol/L), confirmed through comprehensive medical records. The control group comprised age-matched individuals with normal Hcy levels.

2.2. Cell culture and treatment

Human aortic endothelial cells (HAECs, PCS-100-011, ATCC, USA) were meticulously cultured in Vascular Cell Basal Medium (PCS-100-030, ATCC, USA). These cells were nurtured under precise conditions within a humidified incubator set at 37°C, with a controlled atmosphere of 5% CO_2. Subsequently, HAECs underwent treatments with a spectrum of Hcy concentrations (0, 50, 100, 200 μM, H-116-50, GoldBio, USA) for 20 h. Among them, 100 μM was employed to induce HHcy conditions. Additionally, HAECs were exposed to specific agents including Anti-CXCL10 antibodies (701225, Invitrogen, USA), Anti-CXCR3 antibodies (ab71864, Abcam, UK), IgG control antibodies (31154, Thermo Fisher, USA), NBI-74330 (a CXCR3 inhibitor, 4528, Tocris Bioscience, UK), and CXCL10 agonist (266-IP, R&D Systems, USA). These treatments aimed to dissect the mechanistic underpinnings of Hcy-induced endothelial dysfunction and the role of the CXCL10/CXCR3 axis in this process.

2.3. Assessment of plasma levels of Hcy

The plasma levels of Hcy were measured using Homocysteine Assay Kit (MAK354, Sigma-Aldrich, USA). In summary, a precise 1x solution of the Homocysteine Enzyme Mix was meticulously prepared by diluting the reconstituted 10x stock with Homocysteine Assay Buffer (without DTT) in a 10-fold manner. For each dedicated test sample and standard curve reaction, 30 μL of the 1x Homocysteine Enzyme Mix was thoughtfully dispensed into their respective wells, while the wells designated for sample background controls received 30 μL of Homocysteine Assay Buffer (without DTT). Following thorough mixing, the plate was gently incubated at room temperature for 5 minutes, taking care to shield it from light. Concurrently, we prepared the Fluorogenic Developer Mix by expertly combining 30 μL of Fluorogenic Probe Solution with 20 μL of Developer Solution for each individual reaction well, and this mix was immediately added to all wells. Subsequently, the plate was incubated for 15 minutes at room temperature with continuous shaking. The fluorescence emanating was quantified in endpoint mode at λex = 658 nm/λem = 708 nm to determine homocysteine levels in accordance with assay specifications.

2.4. Cell counting Kit-8 (CCK-8) assay

Cell viability was evaluated using the Cell Counting Kit-8 (CCK-8) provided by Dojindo Molecular Technologies, Inc. (CK04-11, Dojindo, USA). In a nutshell, a 100 μL cell suspension was dispensed into each well of a 96-well plate and pre-incubated in a humidified incubator. Subsequently, 10 μL of the CCK-8 solution was introduced into every well of the plate. The plate was then incubated at a temperature of 37°C for a duration of 2 hours. After this incubation period, the absorbance at 450 nm was meticulously measured using a microplate reader.

2.5. Transwell assay

In the Transwell assay, Transwell inserts (3422, Corning, USA) furnished with polycarbonate membranes featuring an 8.0-μm pore size were employed. Within the upper chamber, HAECs were carefully suspended in serum-free medium, while the lower chamber was stocked with culture medium enriched with 10% fetal bovine serum (FBS) as an enticing chemoattractant. The cells were granted a 24-hour migration period at a temperature of 37°C within a humidified incubation environment characterized by a 5% CO_2 atmosphere. Following this migration timeframe, meticulous removal of cells residing on the upper side of the membrane was carried out using cotton swabs. Meanwhile, the migrated cells on the lower side were subjected to a fixation process involving 4% paraformaldehyde, followed by staining with crystal violet (0.5% in 25% methanol, C0775, Sigma-Aldrich, USA). Precise quantification of the migrated cells was conducted under the scrutiny of a light microscope (Olympus, Japan), encompassing five randomly selected fields within each well.

2.6. Wound healing assay

Confluence at 70% was attained by seeding HAECs in 6-well plates. A sterile pipette tip (PT-200, USA Scientific, USA) was used to create a standardized cell-free "wound" or scratch across the cell monolayer. The scratched cells were washed gently with phosphate-buffered saline (PBS) to remove debris and replenished with fresh serum-free medium. Images of the scratch were captured at 0 hours and 24 hours using an inverted microscope (Olympus, Japan) equipped with a camera. The extent of wound closure was quantified by measuring the reduction in scratch width over time.

2.7. Tube formation assay

Plates were pre-coated with growth factor-reduced Matrigel (356231, Corning, USA). Growth factor-reduced Matrigel was thawed on ice, diluted 1:1 with serum-free medium, and added to each well to create a uniform layer. HAECs were then seeded onto the Matrigel-coated wells. Tube-like structures formed by HAECs were visualized

using an inverted microscope and quantified for parameters.

2.8. Western blot

HAECs were initially lysed using RIPA lysis buffer, and the resulting protein lysates were quantified using the BCA Protein Assay Kit (23225, Thermo Fisher, USA). Subsequently, protein samples were subjected to SDS-PAGE on gels with varying acrylamide concentrations, followed by the transfer of separated proteins onto a nitrocellulose or PVDF membrane. Immunoblotting ensued with an overnight incubation with primary antibodies against ICAM-1 (ab282575, Abcam, UK), VCAM-1 (ab134047, Abcam, UK) and β-actin (ab8226, Abcam) at 1: 1000. After washing, the membrane was exposed to HRP-conjugated secondary antibody (ab96879, Abcam, UK), followed by chemiluminescent detection using SuperSignal™ West Pico PLUS Chemiluminescent Substrate (34580, Thermo Fisher, USA). Captured images of chemiluminescent bands were analyzed to quantify the expression levels of ICAM-1 and VCAM-1, with normalization to a loading control.

2.9. Animal model

Male C57BL/6 mice, aged 6 weeks and weighing between 20 and 25 grams, were housed under controlled conditions in our animal facility. The maintenance of the environment included the provision of a 12-hour light/dark cycle, a temperature range of 22–24°C, and humidity levels within the range of 50–60%. The mice were given free access to standard rodent chow and water throughout the study and were acclimated for at least one week before the experiments began. Subsequently, they were allocated into three groups, each comprising 6 mice: the control group received intraperitoneal (i.p.) injections of PBS-DMSO for one month, administered once every two days; the HHcy group consumed a 2% (m/v-1) methionine solution in their drinking water for a duration of two months, in conjunction with i.p. injections of the vehicle; and the HHcy + NBI-74330 group followed the same methionine regimen for two months, supplemented by i.p. injections of NBI-74330 (100 mg/kg) once every two days for one month. Following the final administration, mice were humanely anesthetized and euthanized using 4% chloral hydrate (400 mg/kg) with i.p. injections. Plasma and thoracic aorta samples were then meticulously collected for subsequent experimental analyses.

2.10. Immunohistochemistry (IHC) staining

Paraffin-embedded tissue sections (4 μm thickness) were deparaffinized, subjected to heat-induced epitope retrieval using a microwave, and blocked with 5% bovine serum albumin (BSA) in phosphate-buffered saline (PBS). Primary antibodies targeting ICAM-1 (ab171123, Abcam, UK), VCAM-1 (ab115135, Abcam, UK), CD45 (PA1396, Boster Bio, USA), CD3 (600-020, Thermo Fisher, USA), CD20 (MAB160, Bio-Techne, USA), CD68 (ab125047, Abcam, UK), CXCL10 (10937-1-AP, Proteintech, USA), and CXCR3 (26756-1-AP, Proteintech, USA) were incubated overnight at 4°C. After washing, secondary antibodies (ab97046, Abcam, UK) were applied for 1 hour. Diaminobenzidine (DAB) staining using DAB substrate kit (003836, Bioenno Lifesciences, USA) was performed, followed by counterstaining with hematoxylin (411165000, Thermo Fisher, USA). Imaging was performed using a light microscope (Olympus, Japan).

2.11. Enzyme-linked immunosorbent assay (ELISA) for cytokine detection

ELISA assays for TNF-α, IL-6, and IL-1β were performed using the following kits purchased from Invitrogen (USA): TNF-α Mouse ELISA Kit (BMS607-3), IL-6 Mouse ELISA Kit (BMS603-2), IL-1β Mouse ELISA Kit (BMS6002). Mice serum samples were kept frozen at -80°C until required. In summary, 50 μL of serum was introduced into the wells of pre-coated 96-well plates. These plates were then subjected to a 2-hour incubation at room temperature with gentle agitation. Following this incubation, the wells were washed four times with wash buffer. Subsequently, 100 μL of biotinylated detection antibody was added to each well, and the plates were incubated for an additional 1-hour period at room temperature. After another series of four washes, 100 μL of Streptavidin-HRP was administered to each well, and the plates were incubated for 30 minutes at room temperature. Following further washing, 100 μL of TMB One-Step Substrate Reagent was dispensed into each well, and the plates were left to incubate in the dark for 30 minutes at room temperature. The reaction was halted by the addition of 50 μL of Stop Solution to each well, and the absorbance at 450 nm was determined using a microplate reader.

2.12. Quantitative reverse transcription polymerase chain reaction (qRT-PCR)

Total RNA was extracted from cells or tissues using the RNAeasy Mini Kit (74104, QIAGEN, USA), followed by cDNA synthesis using SuperScript IV Reverse Transcriptase (18090010, Thermo Fisher, USA). Gene-specific primers for CXCL10 and CXCR3 were designed and synthesized, and qPCR reactions were set up with SYBR Green PCR Master Mix (4312704, Thermo Fisher, USA). Thermal cycling was performed using a QuantStudio 3 thermal cycler (Thermo Fisher, USA), and fluorescence signals were collected to monitor amplification. Gene expression levels were determined relative to GAPDH using the $2^{-\Delta\Delta Ct}$ method. Primers used were: CXCL10: Forward Sequence: GGTGAGAAGAGATGTCTGAATCC; Reverse Sequence: GTCCATCCTTGGAAGCACTGCA, CXCR3: Forward Sequence: TACGATCAGCGCCTCAATGCCA; Reverse Sequence: AGCAGGAAACCAGCCACTAGCT, GAPDH: Forward Sequence: ACCAGGGAGGCTGCAGTCC; Reverse Sequence: TCAGTTCGGAGCCCACACGC.

2.13. Statistical analysis

Statistical significance assessments for intergroup differences were conducted using suitable tests, including t-tests or analysis of variance (ANOVA), followed by post-hoc tests when warranted. A significance threshold of 0.05 was applied. GraphPad Prism was employed for all statistical analyses. Error bars in graphical presentations generally denote the standard error of the mean (SEM) or standard deviation (SD) as explicitly indicated.

3. Results

3.1. Hcy induced endothelial dysfunction by inhibiting cell migration and angiogenesis

In this study, the impact of Hcy on endothelial cell

function was investigated. Firstly, elevated Hcy levels were observed in patient serum compared to healthy controls, highlighting its clinical relevance (Figure 1A). Subsequently, various concentrations of Hcy (0, 50, 100, 200 μM) were applied to HAECs. A dose-dependent inhibitory effect on HAEC viability was demonstrated, with higher concentrations resulting in decreased cell vitality, as indicated by CCK8 assays (Figure 1B). Furthermore, endothelial cell migration was significantly impeded by Hcy, as demonstrated by Transwell and scratch assays, thus diminishing their ability to traverse barriers and contribute to vascular repair processes (Figures 1C, D). Moreover, angiogenesis was shown to be reduced by Hcy, as indicated by tube formation assays, suggesting a critical role for Hcy in vascular network formation modulation (Figure 1E). Additionally, upregulation of adhesive protein expression in response to Hcy treatment was revealed by Western blot analysis, implying that Hcy-induced adhesive protein expression may exacerbate HAEC damage (Figure 1F). These results collectively underscored the adverse effects of elevated Hcy levels on endothelial cell function, potentially contributing to endothelial dysfunction and impaired vascular homeostasis.

3.2. HHcy-induced vascular inflammation

A murine model of hyperhomocysteinemia (HHcy) was constructed through a high methionine, low vitamin diet to investigate the influence of HHcy on vascular inflammation. Initially, an increase in serum homocysteine levels was detected in mice exposed to this dietary regimen, confirming HHcy induction (Figure 2A). Subsequently, IHC analysis of the mouse aorta revealed an upregulation of adhesion molecule expression (ICAM-1 and VCAM-1), indicating that HHcy promotes endothelial cell damage (Figure 2B). Further examination of serum samples via enzyme-linked immunosorbent assay (ELISA) demonstrated elevated levels of pro-inflammatory cytokines (TNF-α, IL-6, IL-1β) in the HHcy group compared to the control group, underscoring the pro-inflammatory effects of HHcy (Figure 2C). In addition, IHC analysis of the aorta showed a notable increase in the number of leukocytes in the

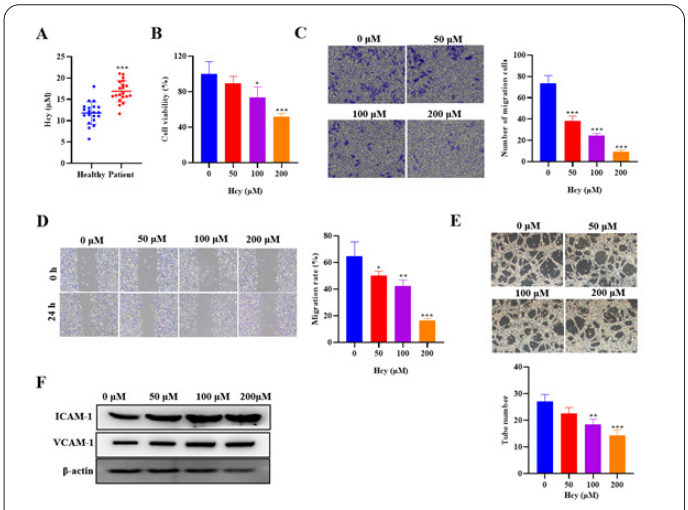

Fig. 1. (A) Levels of Hcy in patient serum. (B) HAECs treated with different concentrations of Hcy (0, 50, 100, 200 μM). (C) Transwell assays assessing cell migration. (D) Wound healing assays examining cell migration. (E) Tube formation assays assessing angiogenesis. (F) Western blot analysis of adhesion molecule expression.

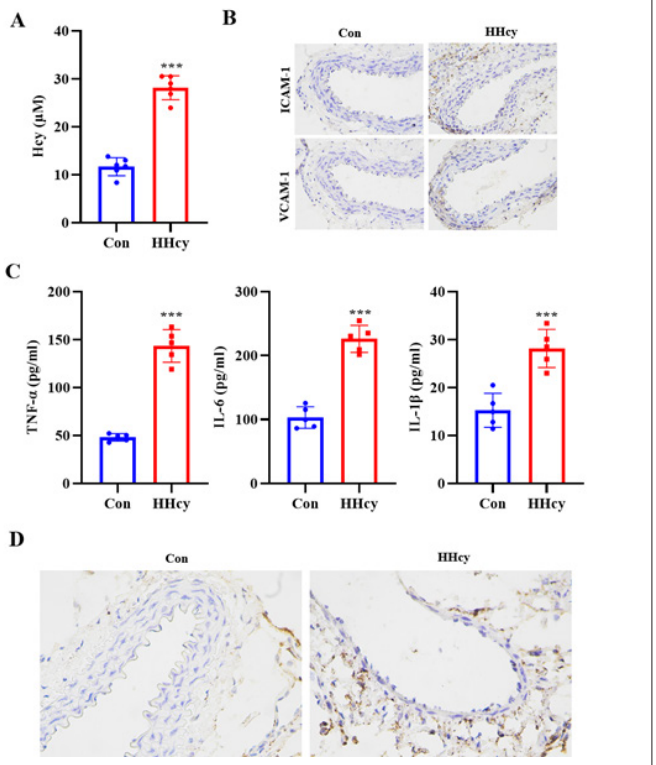

Fig. 2. (A) Levels of Hcy in mice serum in HHcy and Con groups. (B) IHC analysis of the mouse aorta detecting adhesion molecule expression. (C) ELISA analysis of pro-inflammatory cytokines in mice serum. (D) IHC analysis of leukocyte counts in the aorta.

HHcy group, further confirming the promotion of vascular inflammation by HHcy (Figure 2D). Collectively, these findings emphasized the role of HHcy in initiating vascular inflammation and suggested its potential contribution to endothelial dysfunction.

3.3. Hcy induced increased CXCL10/CXCR3 expression in vitro and in vivo

In this study, the influence of Hcy on CXCL10 and CXCR3 expression was investigated both in vitro and in vivo. A dose-dependent upregulation of CXCL10 and CXCR3 expression was observed in HAECs when exposed to varying concentrations of Hcy (0, 50, 100, 200 μM), with higher concentrations correlating with increased expression levels, as presented by qRT-PCR and Western blot analyses (Figures 3A, B). Moreover, IHC analysis of the aorta in HHcy mice demonstrated a notable upregulation in CXCL10 and CXCR3 expression compared to the control group, further confirming the in vivo impact of HHcy on these chemokines and their receptor (Figure 3C). Moreover, examination via qRT-PCR of arterial endothelial cells unveiled a significant upregulation in CXCL10 and CXCR3 expression within the HHcy group in comparison to the control group (Figure 3D). These findings collectively emphasize the influence of Hcy in promoting heightened CXCL10 and CXCR3 expression, both in in vitro and in vivo settings, thus emphasizing its potential contribution to the regulation of endothelial function and vascular responses.

3.4. Inhibition of CXCL10 or CXCR3 resists homocysteine-induced vascular damage

In this study, the impact of inhibiting CXCL10 or CXCR3 on Hcy-induced vascular damage was explored

in a comparative analysis of the Con group, Hcy group, Hcy+Anti-CXCL10 group, and Hcy+Anti-CXCR3 group. Cell viability assessed through CCK8 assays indicated that Hcy suppressed HAEC vitality, whereas the introduction of CXCL10 or CXCR3 neutralizing antibodies restored this impact (Figure 4A). Transwell and wound healing assays further corroborated the inhibitory effect of Hcy on HAEC migration, as presented by number of migration cells and migration rate, and demonstrated that neutralizing antibodies against CXCL10 or CXCR3 augmented HAEC migration ability (Figures 4B, C). Western blot analysis revealed increased expression of adhesion molecules (VCAM-1 and ICAM-1) in Hcy + IgG group, which was however rescued in Hcy+Anti-CXCL10 group and Hcy+Anti-CXCR3 group, suggesting that Hcy regulated HAEC damage through CXCL10 or CXCR3 (Figure 4D). Moreover, tube formation assay detected suppressed angiogenesis in Hcy + IgG group and relatively increased one in neutralizing antibody group (Figure 4E). Collectively, these findings underscored that Hcy-induced vascular damage can be mitigated by the inhibition of CXCL10 or CXCR3, highlighting their potential as therapeutic targets for countering endothelial dysfunction.

3.5. Blocking the CXCL10/CXCR3 pathway affected endothelial cell function

In this study, the impact of CXCR3 inhibition using the inhibitor NBI-74330 on endothelial cell function was investigated, with comparisons made among three experimental groups: Con group, CXCL10 group, and CXCL10+NBI-74330 group. Cell viability, as assessed by CCK8 assays, revealed a suppression in the CXCL10 group, while the CXCL10+NBI-74330 group demonstrated the restoration of reduced cell viability (Figure 5A). Transwell assays indicated reduced number of migrated cells in the CXCL10 group, whereas the CXCL10+NBI-74330 group exhibited a restoration (Figure 5B). Western blot demonstrated increased expression of adhesion molecules (ICAM-1 and VCAM-1) in the CXCL10 group, while the

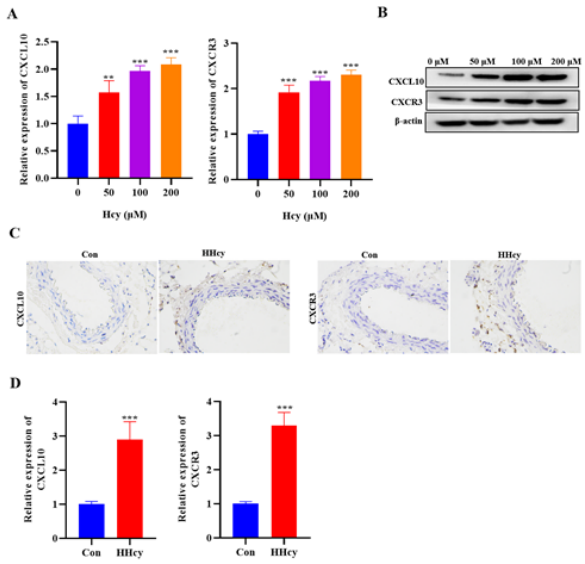

Fig. 3. (A, B) qRT-PCR and Western blot analysis of CXCL10 and CXCR3 expression in HAECs treated with different concentrations of Hcy. (C) IHC analysis of the aorta in HHcy mice showing CXCL10 and CXCR3 expression. (D) qRT-PCR analysis of CXCL10 and CXCR3 expression in arterial endothelial cells.

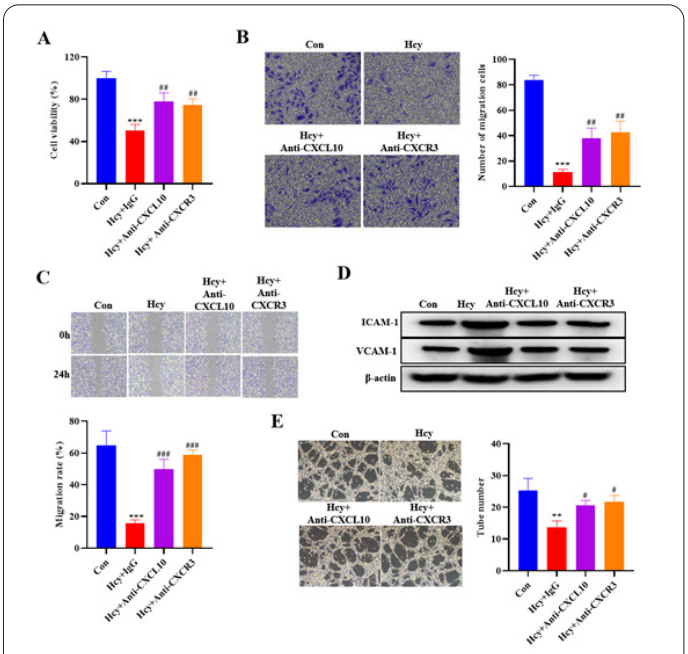

Fig. 4. (A) CCK8 assays assessing cell viability. (B, C) Transwell and wound healing assays examining cell migration. (D) Western blot analysis of adhesion molecules expression. (E) Tube formation assays assessing angiogenesis.

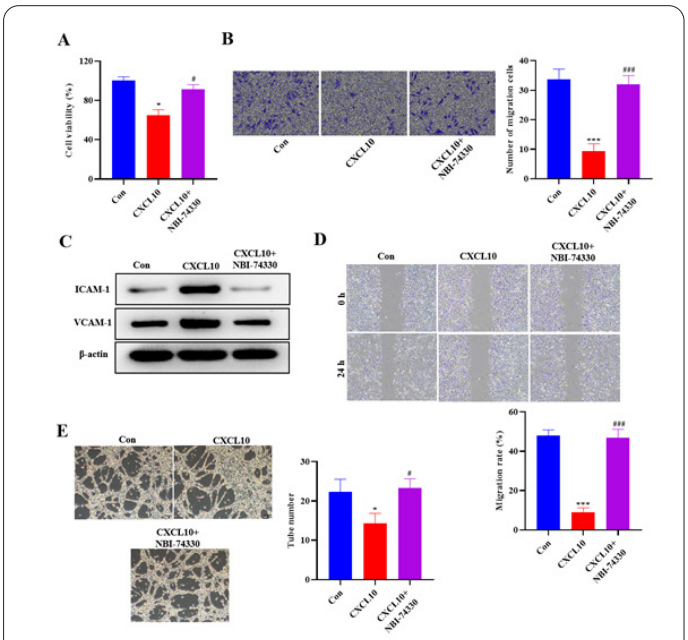

Fig. 5. (A) CCK8 assays measuring cell viability. (B) Transwell assays assessing cell migration. (C) Western blot analysis of adhesion molecules expression (ICAM-1 and VCAM-1). (D) Wound healing assays measuring migration rate. (E) Tube formation assays evaluating angiogenesis.

CXCL10+NBI-74330 group showed a restoration (Figure 5C). Wound healing assay measuring migration rate revealed a decrease in the CXCL10 group, with a subsequent restoration observed in the CXCL10+NBI-74330 group (Figure 5D). Furthermore, tube formation assays showed suppressed angiogenesis in the CXCL10 group, with a restoration of diminished angiogenesis observed in the CXCL10+NBI-74330 group (Figure 5E). Collectively, these findings confirmed that exogenous CXCL10 protein could inhibit endothelial cell proliferation and migration. Furthermore, the use of the CXCR3 inhibitor NBI-74330

can reverse these effects, providing evidence of the regulatory role of the CXCL10/CXCR3 axis in HAEC function.

3.6. Injection of NBI-74330 alleviates inflammation in HHcy mice

In this study, the impact of tail vein injection of the CXCR3 inhibitor NBI-74330 on inflammation in HHcy mice was investigated, comparing two experimental groups: HHcy group and HHcy+NBI-74330 group. Measurement of Hcy levels in mouse serum revealed a decrease in the HHcy+NBI-74330 group (Figure 6A). IHC analysis of mouse aortas demonstrated reduced adhesion molecules protein expression in the HHcy+NBI-74330 group (Figure 6B). ELISA analysis of pro-inflammatory cytokines (TNF-α, IL-6, IL-1β) in serum showed a decrease in the HHcy+NBI-74330 group (Figure 6C). IHC analysis of leukocyte counts in the aorta indicated a decrease in the HHcy+NBI-74330 group (Figure 6D). These results collectively indicated that the injection of NBI-74330 led to a reduction in serum Hcy levels and a decrease in vascular inflammation in HHcy mice.

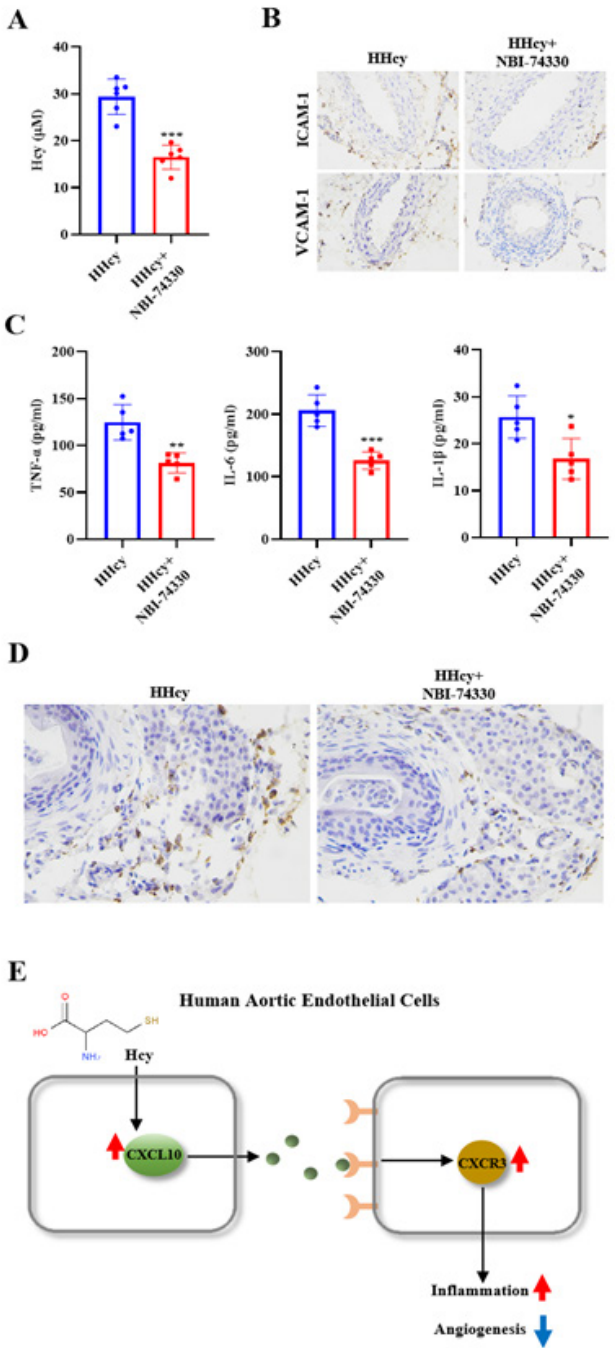

Fig. 6. (A) Levels of Hcy in HHcy mice serum. (B) IHC analysis of adhesion molecules in mouse aortas. (C) ELISA analysis of pro-inflammatory cytokines in serum. (D) IHC analysis of leukocyte counts in the aorta. (E) Hcy in Human Aortic Endothelial Cells.

4. Discussion

Our study comprehensively examined the impact of Hcy on endothelial function, revealing significant implications for vascular health. As demonstrated, Hcy exerted detrimental effects on endothelial cell viability, migration, and angiogenesis. Furthermore, our inquiry unveiled that HHcy precipitates vascular inflammation, as indicated by heightened serum levels of pro-inflammatory cytokines and an augmented count of white blood cells within the aorta. These findings resonate with previous research. A recent review of the literature reveals a significant correlation between elevated Hcy levels and endothelial dysfunction. HHcy, defined as fasting plasma Hcy levels exceeding 15 μmol/L, is identified as a critical risk factor for atherosclerosis (AS), promoting its development and the occurrence of cardiovascular events [15]. This condition is also directly and indirectly associated with cerebral small vessel disease (cSVD), with endothelial dysfunction playing a pivotal role [16]. Furthermore, increased Hcy levels have been linked to atherosclerosis in healthy individuals, reinforcing the detrimental impact of elevated Hcy on vascular health [17]. The disruption of Hcy metabolism is shown to contribute to endothelial dysfunction and atherosclerosis [18]. HHcy's harmful effects extend to renal function as well, where it reduces nitric oxide utilization, increases oxidative stress, induces endothelial dysfunction, and promotes vascular smooth cell proliferation [19].

The intricate relationship was highlighted between Hcy and the CXCL10/CXCR3 axis, demonstrating that Hcy could modulate the expression of CXCL10 and CXCR3 in both in vitro and in vivo settings. Additionally, we explored interventions aimed at mitigating Hcy-induced vascular damage. The experiments involving CXCR3 inhibition through NBI-74330 provided further support for the efficacy of this approach in reversing Hcy-induced endothelial cell dysfunction. This is consistent with previous studies that have shown the therapeutic potential of targeting the CXCL10/CXCR3 axis. For instance, the interplay of the CXCL9, CXCL10, CXCL11/CXCR3 axis, along with the involvement of G protein-coupled receptor kinase 2 (GRK2), has been linked to a myriad of processes within the realms of inflammation and immunity [20, 21]. The CXCL10/CXCR3 signaling pathway, renowned for its regulatory role in immune cell differentiation, migration, and infiltration, exerts a far-reaching impact on phenomena like tumor progression and metastasis [22]. Interestingly, CXCL10 has exhibited its capacity to attract regulatory T cells (Tregs) to the liver via their surface receptor CXCR3, while also playing a pivotal role in mechanisms underlying pain perception [23]. Moreover, CXCL10 engages its receptor CXCR3, fine-tuning immune responses by orchestrating the recruitment of a diverse array of leukocytes, encompassing T cells and monocytes/macrophages [24]. Pertinently, as a potential therapeutic avenue, the blockade of the CXCR3/CXCL10 axis has displayed promise in mitigating inflammation stemming from disruptions in immunoproteasome function [25], and CXCR3 inhibition

by AMG487 has been found to enhance autophagy and reduce the inflammatory response [26]. In conclusion, our results not only corroborated previous findings but also contributed new insights specifically in the context of Hcy and the CXCL10/CXCR3 axis.

Based on intervention with NBI-74330, we dig further into its therapeutic impact on impairing endothelial function. It was shown that the injection of NBI-74330 alleviated inflammation in HHcy mice. Such findings aligned with existing literature on the therapeutic potential of CXCR3 inhibition. For instance, one study reported that the inhibition of the CXCR3/CXCL10 axis effectively alleviated inflammation induced by immunoproteasome dysfunction [27]. Additionally, another study demonstrated that blocking the CXC chemokine receptor 3 (CXCR3) resulted in reduced inflammation and enhanced survival in a murine model of nearly lethal polymicrobial sepsis [28]. This further supported our results, suggesting that CXCR3 inhibition could be a promising therapeutic strategy for conditions associated with inflammation.

In conclusion, our study illuminated the multifaceted effects of Hcy on endothelial function, with specific attention to HHcy-induced vascular inflammation. Additionally, we emphasized the regulatory role Hcy plays in the CXCL10/CXCR3 axis and the potential therapeutic significance of targeting this axis in the management of endothelial dysfunction. Future studies should delve into the clinical applicability of CXCR3 inhibition as a treatment strategy for conditions associated with elevated Hcy levels, such as cardiovascular diseases and atherosclerosis.

Informed Consent

The authors report no conflict of interest.

Availability of data and material

We declared that we embedded all data in the manuscript.

Authors' contributions

XY conducted the experiments and wrote the paper; XY, YZ and HD analyzed and organized the data; SX conceived, designed the study and revised the manuscript.

Funding

This work was supported by the National Natural Science Foundation of China (No. 82160084), and the Jiangxi Provincial Natural Science Foundation (No. 20181BAB215003).

Acknowledgement

We thanked the The Second Affiliated Hospital of Nanchang University for approving our study.

References

1. Hasty R, Smolar EN (2002) Homocysteine. Compr Ther 28(1):34–38. doi: 10.1007/s12019-002-0040-x
2. Zhao W, Gao F, Lv L, Chen X (2022) The interaction of hypertension and homocysteine increases the risk of mortality among middle-aged and older population in the United States. J Hypertens 40(2):254–263. doi: 10.1097/hjh.0000000000003002
3. Paganelli F, Mottola G, Fromonot J, Marlinge M, Deharo P, Guieu R, Ruf J (2021) Hyperhomocysteinemia and cardiovascular disease: is the adenosinergic system the missing link? Int J Mol Sci 22(4):1690. doi: 10.3390/ijms22041690
4. Dong B, Wu R (2020) Plasma homocysteine, folate and vitamin B12 levels in Parkinson's disease in China: A meta-analysis. Clin Neurol Neurosurg 188:105587. doi: 10.1016/j.clineuro.2019.105587
5. Zhou S, Chen J, Cheng L, Fan K, Xu M, Ren W, et al (2021) Age-dependent association between elevated homocysteine and cognitive impairment in a post-stroke population: a prospective study. Front Nutr 8:691837. doi: 10.3389/fnut.2021.691837
6. Liang R, Chen S, Jin Y, Tao L, Ji W, Zhu P, et al (2022) The CXCL10/CXCR3 axis promotes disease pathogenesis in mice upon CVA2 infection. Microbiol Spectr 10(3):e0230721. doi: 10.1128/spectrum.02307-21
7. Lee EY, Lee ZH, Song YW (2009) CXCL10 and autoimmune diseases. Autoimmun Rev 8(5):379–383. doi: 10.1016/j.autrev.2008.12.002
8. Falk MK, Singh A, Faber C, Nissen MH, Hviid T, Sørensen TL (2014) Dysregulation of CXCR3 expression on peripheral blood leukocytes in patients with neovascular age-related macular degeneration. Invest Ophthalmol Vis Sci 55(7):4050–4056. doi: 10.1167/iovs.14-14107
9. Koper OM, Kamińska J, Sawicki K, Kemona H (2018) CXCL9, CXCL10, CXCL11, and their receptor (CXCR3) in neuroinflammation and neurodegeneration. Adv Clin Exp Med 27(6):849–856. doi: 10.17219/acem/68846
10. Moreno Ayala MA, Campbell TF, Zhang C, Dahan N, Bockman A, Prakash V, et al (2023) CXCR3 expression in regulatory T cells drives interactions with type I dendritic cells in tumors to restrict CD8(+) T cell antitumor immunity. Immunity 56(7):1613–1630.e5. doi: 10.1016/j.immuni.2023.06.003
11. Hermann A, Sitdikova G (2021) Homocysteine: biochemistry, molecular biology and role in disease. Biomolecules 11(5):737. doi: 10.3390/biom11050737
12. Moll S, Varga EA (2015) Homocysteine and MTHFR mutations. Circulation 132(1):e6–e9. doi: 10.1161/circulationaha.114.013311
13. Undas A, Brozek J, Szczeklik A (2005) Homocysteine and thrombosis: from basic science to clinical evidence. Thromb Haemost 94(5):907–915. doi: 10.1160/th05-05-0313
14. Chen Y, Liu R, Zhang G, Yu Q, Jia M, Zheng C, et al (2015) Hypercysteinemia promotes atherosclerosis by reducing protein S-nitrosylation. Biomed Pharmacother 70:253–259. doi: 10.1016/j.biopha.2015.01.030
15. Yuan D, Chu J, Lin H, Zhu G, Qian J, Yu Y, et al (2023) Mechanism of homocysteine-mediated endothelial injury and its consequences for atherosclerosis. Front Cardiovasc Med 9:1109445. doi: 10.3389/fcvm.2022.1109445
16. Li S, Li G, Luo X, Huang Y, Wen L, Li J (2021) Endothelial dysfunction and hyperhomocysteinemia-linked cerebral small vessel disease: underlying mechanisms and treatment timing. Front Neurol 12:736309. doi: 10.3389/fneur.2021.736309
17. Obradovic M, Zaric BL, Haidara MA, Isenovic ER (2018) Link between homocysteine and cardiovascular diseases. Curr Pharmacol Rep 4:1–9. doi: 10.1007/s40495-017-0119-9
18. Esse R, Barroso M, Tavares de Almeida I, Castro R (2019) The contribution of homocysteine metabolism disruption to endothelial dysfunction: state-of-the-art. Int J Mol Sci 20(4):867. doi: 10.3390/ijms20040867
19. Wang YN, Xia H, Song ZR, Zhou XJ, Zhang H (2022) Plasma homocysteine as a potential marker of early renal function decline in IgA nephropathy. Front Med (Lausanne) 9:812552. doi: 10.3389/fmed.2022.812552
20. Zhang J, Zhang X, Shi X, Liu Y, Cheng D, Tian Q, et al (2023) CXCL9, 10, 11/CXCR3 axis contributes to the progress of primary sjogren's syndrome by activating GRK2 to promote T lymphocyte migration. Inflammation 46(3):1047–1060. doi: 10.1007/

s10753-023-01791-9

21. Pan M, Wei X, Xiang X, Liu Y, Zhou Q, Yang W (2023) Targeting CXCL9/10/11–CXCR3 axis: an important component of tumor-promoting and antitumor immunity. Clin Transl Oncol 25(8):2306–2320. doi: 10.1007/s12094-023-03126-4
22. Li CX, Ling CC, Shao Y, Xu A, Li XC, Ng KT, et al (2016) CXCL10/CXCR3 signaling mobilized-regulatory T cells promote liver tumor recurrence after transplantation. J Hepatol 65(5):944–952. doi: 10.1016/j.jhep.2016.05.032
23. Ye D, Bu H, Guo G, Shu B, Wang W, Guan X, et al (2014) Activation of CXCL10/CXCR3 signaling attenuates morphine analgesia: involvement of Gi protein. J Mol Neurosci 53(4):571–579. doi: 10.1007/s12031-013-0223-1
24. Lee JH, Kim B, Jin WJ, Kim HH, Ha H, Lee ZH (2017) Pathogenic roles of CXCL10 signaling through CXCR3 and TLR4 in macrophages and T cells: relevance for arthritis. Arthritis Res Ther 19(1):163. doi: 10.1186/s13075-017-1353-6
25. Satarkar D, Patra C (2022) Evolution, expression and functional analysis of CXCR3 in neuronal and cardiovascular diseases: a narrative review. Front Cell Dev Biol 10:882017. doi: 10.3389/fcell.2022.882017
26. Zhang C, Deng Y, Zhang Y, Ba T, Niu S, Chen Y, et al (2023) CXCR3 inhibition blocks the NF-κB signaling pathway by elevating autophagy to ameliorate lipopolysaccharide-induced intestinal dysfunction in mice. Cells 12(1):182. doi: 10.3390/cells12010182
27. Sasaki Y, Arimochi H, Otsuka K, Kondo H, Tsukumo SI, Yasutomo K (2022) Blockade of the CXCR3/CXCL10 axis ameliorates inflammation caused by immunoproteasome dysfunction. JCI Insight 7(7):e152681. doi: 10.1172/jci.insight.152681
28. Delano MJ, Moldawer LL (2012) CXCR3 blockade: a novel antisepsis approach? Crit Care 16(6):176. doi: 10.1186/cc11818